Dmytro Ivaneyko, Vladimir Toshchevikov, Marina Saphiannikova, Gert Heinrich

Mechanical properties of magneto-sensitive elastomers: unification of the continuummechanics and microscopic theoretical approaches

Erstveröffentlichung in / First published in:
Soft Matter. 2014, 10(13), S. 2213–2225 [Zugriff am: 04.11.2019]. Royal Society of Chemistry. ISSN 1744-6848.

DOI: https://doi.org/10.1039/c3sm52440j

Soft Matter

PAPER

View Article Online
View Journal | View Issue

Cite this: *Soft Matter*, 2014, **10**, 2213

Mechanical properties of magneto-sensitive elastomers: unification of the continuum-mechanics and microscopic theoretical approaches

Dmytro Ivaneyko,[ab] Vladimir Toshchevikov,[ac] Marina Saphiannikova*[a] and Gert Heinrich[ab]

Received 16th September 2013
Accepted 20th December 2013

DOI: 10.1039/c3sm52440j

www.rsc.org/softmatter

A new theoretical formalism is developed for the study of the mechanical behaviour of magneto-sensitive elastomers (MSEs) under a uniform external magnetic field. This formalism allows us to combine macroscopic continuum-mechanics and microscopic approaches for complex analysis of MSEs with different shapes and with different particle distributions. It is shown that starting from a model based on an explicit discrete particle distribution one can separate the magnetic field inside the MSE into two contributions: one which depends on the shape of the sample with finite size and the other, which depends on the local spatial particle distribution. The magneto-induced deformation and the change of elastic modulus are found to be either positive or negative, their dependences on the magnetic field being determined by a non-trivial interplay between these two contributions. Mechanical properties are studied for two opposite types of coupling between the particle distribution and the magneto-induced deformation: absence of elastic coupling and presence of strong affine coupling. Predictions of a new formalism are in a qualitative agreement with existing experimental data.

1 Introduction

Composites that consist of a polymer matrix and magnetic inclusions belong to a class of smart materials, whose mechanical behavior can be controlled by application of an external magnetic field. Magneto-sensitive elastomers (MSEs) are one of the very promising classes among these smart materials. Nowadays, MSEs find a wide range of industrial applications as controllable membranes, adaptive tuned vibration absorbers, stiffness tunable mounts and automobile suspensions.[1]

Different types of magnetic particles can be used as fillers in MSEs. Mostly carbonyl iron is used; it is dictated by commercial interests.[2] Carbonyl iron particles produced industrially can have almost mono-dispersed size around 1 μm, shape close to spherical and show soft magnetic behaviour. The spatial distribution of particles inside an elastomer can be either isotropic or anisotropic (chain-like, plane-like), depending on the method of preparation.[3] The particle distribution significantly affects the mechanical properties of MSE under a uniform external magnetic field. Especially the spatial distribution of magnetic particles influences the sign of magneto-induced deformation (contraction or expansion, usually considered as magnetostriction) and the mechanical moduli (softening or stiffening). Many experiments show that MSEs with an isotropic particle distribution demonstrate a uniaxial expansion along the magnetic field,[4,5] while MSEs with a chain-like particle distribution demonstrate a uniaxial contraction along the magnetic field.[4,6,7] Besides, most of these studies indicate increase of the elastic modulus[8–11] and shear modulus[12–23] with increasing magnetic field for both isotropic and anisotropic MSEs.

At the same time a lot of theoretical studies have been proposed to investigate the mechanical behaviour of MSEs under a uniform external magnetic field.[5,6,24–29] These studies are based on two approaches: macroscopic continuum-mechanics approach[5,24–26] and microscopic approach.[6,27–30] The macroscopic continuum-mechanics approach considers the deformation-dependent demagnetizing shape factor and does not take into account a local discrete distribution of particles. It always predicts the elongation of MSEs along the external magnetic field and increase of the elastic modulus. However, the continuum-mechanics approach is not able to describe the effect of particle distribution on the magneto-elastic properties of MSEs.

The microscopic approach considers explicitly the discrete particle distribution inside a polymer matrix. Dipole–dipole interaction between the magnetic particles leads to their pair-wise attraction and repulsion depending on mutual positions of the particles. Since the dipole–dipole interaction is a long-range

[a]*Leibniz-Institut für Polymerforschung Dresden e.V., Hohe Str. 6, 01069 Dresden, Germany. E-mail: grenzer@ipfdd.de; Fax: +49 (0)35 1465 8362; Tel: +49 (0)35 1465 8597*

[b]*Institute of Materials Science, Technical University of Dresden, Helmholtz Str. 7, 01069 Dresden, Germany*

[c]*Institute of Macromolecular Compounds, Russian Academy of Science, Bolshoi Prospect 31, V.O., Saint-Petersburg, 199004, Russia*

interaction, the spatial distribution of particles inside the matrix strongly affects the sign of the magneto-induced deformation and behaviour of tensile and shear moduli.[31,32] The microscopic approach can predict a different sign of magneto-induced deformation (expansion or contraction), depending on the form of spatial particle distribution. However, previous studies by the authors[31,32] as well as quasi-static one-chain models,[6,27,28] the multi-chain model[29] and extension of our approach[31] to the wavy particle-chain structure[30] considered infinite MSE samples and thus neglected the effects of shape change for finite samples. Therefore, a new theoretical approach is needed, which would allow us to describe in agreement with experiments the mechanical properties of MSEs with different shapes and with different particle distributions.

Here we would like to mention recently published studies on the magneto-induced deformation of ferrogels,[33,34] *i.e.* magnetic systems with randomly oriented permanent magnetic moments. In these studies the continuum-mechanics approach was modified phenomenologically to take into account the local particle distribution. The latter was introduced through an equation of the magnetic susceptibility χ of MSEs, assuming that the rearrangement of particle positions provides the change of χ. The method proposed allows consideration of stochastic particle distributions[33] and the chain-like distributions[34] within a ferrogel. It is however restricted to qualitative predictions of a sign of the magneto-induced deformation and does not predict magnitudes of the deformation and the mechanical moduli. Besides, MSEs and ferrogels are totally different magnetic systems in terms of the mechanism of how the particles move and how the magnetic moments orient. Thus, this recent approach[33,34] cannot be applied to MSEs.

The aim of the present work is to develop a new theoretical formalism for the mechanical properties of MSEs with different shapes and with different particle distributions. We show that starting from a model based on an explicit discrete particle distribution one can separate the magnetic field inside the MSE into two contributions: one which depends on the shape of the sample with finite size and the other, which depends on the local particle distribution. Further, we show that the behaviour of magneto-induced deformation and elastic modulus as functions of magnetic field is determined by a non-trivial interplay between these two contributions. For simplicity, we consider in this study a linear regime of magnetisation of the magnetic particles and linear elastic response of the polymer matrix.

2 Magnetic field inside an MSE

2.1 Model and general equations

In this section we focus on calculation of the magnetic field inside an MSE. We introduce a microscopic model of the MSE that allows us to take explicitly into account both the shape of a finite sample and the local spatial distribution of particles. We assume that the MSE sample has the shape of an ellipsoid of revolution (see Fig. 1) with a pair of equal semi-axes ($B = C$) and a distinct third semi-axis (A) which is an axis of symmetry. The sample aspect ratio $\gamma = A/B$ will be used in the next sections to characterize the initial shape of the sample as well as the

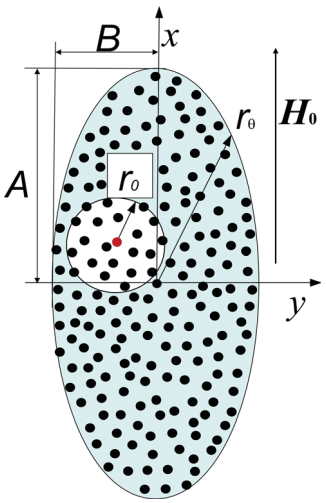

Fig. 1 Schematic drawing of the microscopic model of MSE under a uniform external magnetic field H_0.

sample deformation. In the present section we use γ as a parameter, which defines the shape of a sample: if $\gamma = 1$ then the sample is a sphere, if $\gamma > 1$ then the sample is a prolate ellipsoid and if $\gamma < 1$ then the sample is an oblate ellipsoid. Further, we assume that the MSE consists of a non-magnetic elastomeric matrix with embedded magnetic particles. All magnetic particles are prepared from the same material with the magnetic susceptibility χ ($\chi \gg 1$). For simplicity it is assumed that the particles have the same spherical form of radius R. In the present section we derive general equations for the magnetic field inside an MSE with an arbitrary spatial distribution of particles. In the next sections these equations will be applied to concrete (regular) particle distributions.

Application of a homogeneous magnetic field $\mathbf{H}_0$ to the MSE causes magnetization of embedded particles. In our work we consider such a configuration where the external magnetic field $\mathbf{H}_0$ is directed along the axis of symmetry (x-axis in Fig. 1). For further calculations we use the result of the continuum-mechanics theory[35] that the homogeneous external magnetic field induces a constant magnetization, which is independent of the position inside the ellipsoidal sample. In accordance with this result, we assume that all particles have the same dipole moment $\mathbf{m}$, which is directed along the x-axis: $\mathbf{m} = \{m, 0, 0\}$. The last assumption implies the homogeneity of a particle distribution, *i.e.* the absence of dense clusters of particles separated by particle-poor regions, as well as a statistically relevant number of particles in a macroscopic sample. The latter condition puts an additional restriction on the volume fraction of particles ϕ, which will be discussed later in Section 3.

The first step is to calculate the induced magnetic field $\mathbf{H}_d$, which is produced by all surrounding magnetic particles in the point $\mathbf{r}_j$, where the j-th particle is situated. The value of $\mathbf{H}_d$ produced by dipoles $\mathbf{m}$ is given by[31,32]

$$\mathbf{H}_d(\mathbf{r}_j) = \frac{1}{4\pi}\mathbf{m}\sum_{i\neq j}\frac{3(\mathbf{r}_{ji})_x^2 - \mathbf{r}_{ji}^2}{|\mathbf{r}_{ji}|^5}, \quad (1)$$

where $\mathbf{r}_{ji}$ is the radius-vector which connects the j-th and i-th particles. The sum in the right-hand side of eqn (1) is performed over all particles excluding the j-th particle $i \neq j$. One can see from eqn (1) that the field $\mathbf{H}_d$ is determined by the distribution of particles inside the MSE. It is convenient to rewrite eqn (1) in the following form:

$$\mathbf{H}_d(\mathbf{r}_j) = \mathbf{m}cf(\{\mathbf{r}_{ji}\}), \tag{2}$$

where c is the number of particles in the unit volume and the dimensionless function f is determined only by the spatial distribution of particles $\{\mathbf{r}_{ij}\}$:

$$f(\{\mathbf{r}_{ji}\}) = \frac{1}{4\pi c}\sum_{i\neq j}\frac{3(\mathbf{r}_{ji})_x{}^2 - \mathbf{r}_{ji}{}^2}{|\mathbf{r}_{ji}|^5}. \tag{3}$$

Note that the calculation of $\mathbf{H}_d$ represents a very complicated problem which includes a numerical summation over huge number of particles in a macroscopic sample.

Now we will introduce a theoretical formalism which allows us to simplify the numerical calculation of the factor f. For that we split the volume of the sample into two parts: the microsphere of radius r_0 with a center on the j-th particle (red point in Fig. 1) and the remaining part of the macroscopic sample. The value r_0 is chosen to be much larger than an average distance between neighbouring particles R_0: $r_0 \gg R_0 \simeq c^{-1/3}$. Thus, the factor f can be split into two parts:

$$f = f_{\text{micro}} + f_{\text{macro}}, \tag{4}$$

where f_{micro} is a sum over particles inside the microsphere:

$$f_{\text{micro}} = \frac{1}{4\pi c}\sum_{|\mathbf{r}_{ji}|\leq r_0}\frac{3(\mathbf{r}_{ji})_x{}^2 - \mathbf{r}_{ji}{}^2}{|\mathbf{r}_{ji}|^5} \tag{5}$$

and f_{macro} is a sum inside the remaining part of the sample. For $r_0 \gg R_0 \simeq c^{-1/3}$ the sum f_{macro} is well approximated by an integral

$$f_{\text{macro}} = \frac{1}{4\pi}\int_{\Delta V}\frac{3\mathbf{r}_x{}^2 - \mathbf{r}^2}{|\mathbf{r}|^5}\mathrm{d}^3\mathbf{r}, \tag{6}$$

where ΔV is the volume between the microsphere of radius r_0 and the boundary of the ellipsoid. It can be shown that the location of the microsphere does not affect the value of f_{macro}. Performing transformation of the cartesian coordinates $\{x, y, z\}$ to the spherical coordinates $\{r, \theta, \phi\}$:

$$x = r\cos\theta, \quad y = r\sin\theta\cos\phi, \quad z = r\sin\theta\sin\phi, \tag{7}$$

one can calculate the integral in eqn (6) analytically. We rewrite it in the form

$$f_{\text{macro}} = \frac{1}{4\pi}\int_0^{2\pi}\mathrm{d}\phi\int_0^{\pi}\sin\theta\,\mathrm{d}\theta\int_{r_0}^{r_\theta}r^2\mathrm{d}r\frac{3\cos^2\theta - 1}{r^3}, \tag{8}$$

where r_θ defines the boundary of the ellipsoid:

$$r_\theta = \left(\frac{\cos^2\theta}{A^2} + \frac{\sin^2\theta}{B^2}\right)^{-1/2}. \tag{9}$$

After integration over ϕ and r one gets

$$f_{\text{macro}} = \frac{1}{2}\int_0^{\pi}\sin\theta\left(3\cos^2\theta - 1\right)(\ln r_\theta - \ln r_0)\mathrm{d}\theta. \tag{10}$$

The integration of the term, which contains $\ln r_0$, results in zero, since $\int_0^{\pi}\sin\theta(3\cos^2\theta - 1)\mathrm{d}\theta = 0$. Thus, the factor f_{macro} is independent of the microsphere radius r_0 and can be rewritten in the form

$$f_{\text{macro}} = -\frac{1}{2}\int_0^1\left(3\xi^2 - 1\right)\ln\left[\xi^2 + \gamma^2\left(1 - \xi^2\right)\right]\mathrm{d}\xi, \tag{11}$$

where the substitution $\xi = \cos\theta$ was used. Note that $\gamma = A/B$ is the sample aspect ratio. The integration results in the following analytical equations:

$$f_{\text{macro}} = \frac{1}{3} - N(\gamma), \tag{12}$$

where

$$N(\gamma) = \begin{cases} \dfrac{\gamma^{-2}}{(1-\gamma^{-2})^{3/2}}\left[\operatorname{arth}\left(\dfrac{\sqrt{\gamma^2-1}}{\gamma}\right) - \dfrac{\sqrt{\gamma^2-1}}{\gamma}\right], \gamma > 1 \\ 1/3, \qquad\qquad \gamma = 1 \\ \dfrac{\gamma^{-2}}{(\gamma^{-2}-1)^{3/2}}\left[\dfrac{\sqrt{1-\gamma^2}}{\gamma} - \operatorname{arctg}\left(\dfrac{\sqrt{1-\gamma^2}}{\gamma}\right)\right], \gamma < 1 \end{cases} \tag{13}$$

Note that $N(\gamma)$ is exactly the demagnetizing factor N, which appears in the continuum-mechanics theory.[36] One can see that $f_{\text{macro}} = 0$ for $\gamma = 1$.

Hence, the induced magnetic field $\mathbf{H}_d$ is determined as a contribution of two factors f_{micro} and f_{macro}. The factor f_{macro} is defined by the demagnetizing factor $N(\gamma)$ which depends on the shape of the sample but is independent of the particle distribution. The factor f_{micro} is determined by the particle distribution but is independent of the shape of the sample, since the sum in eqn (5) is performed over particles inside a fixed sphere. Note that the sum in eqn (5) converges at $r_0 \gg R_0 \simeq c^{-1/3}$, since any additional sum from the sphere of radius r_0 till a larger sphere with the radius $\tilde{r}$ can be approximated by an integral of the form similar to eqn (10). This integral is equal to zero for $r_\theta = \tilde{r} = \text{const}$, since $\int_0^{\pi}\sin\theta(3\cos^2\theta - 1)\mathrm{d}\theta = 0$. We have found that the sum in eqn (5) converges at $r_0 > 10R_0$.[31]

Thus, the formalism developed above allows us to combine the continuum-mechanics and the microscopic approaches. It takes explicitly into account the effect of the sample shape and the discrete particle distribution. Below, we demonstrate that this formalism provides exact solutions for $\mathbf{H}_d$ using different lattice models.

2.2 Isotropic particle distribution

As in our previous paper[32] we use three different lattice models to mimic the isotropic distribution of magnetic particles: simple cubic (SC), body-centered cubic (BCC) and hexagonal close-packed (HCP) lattices (see Fig. 2).

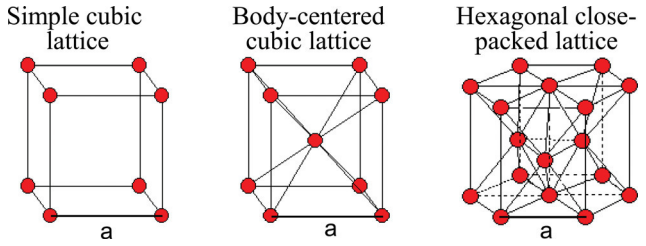

Fig. 2 Three regular lattices to mimic the isotropic spatial distribution of magnetic particles; *a* is the edge of each lattice.

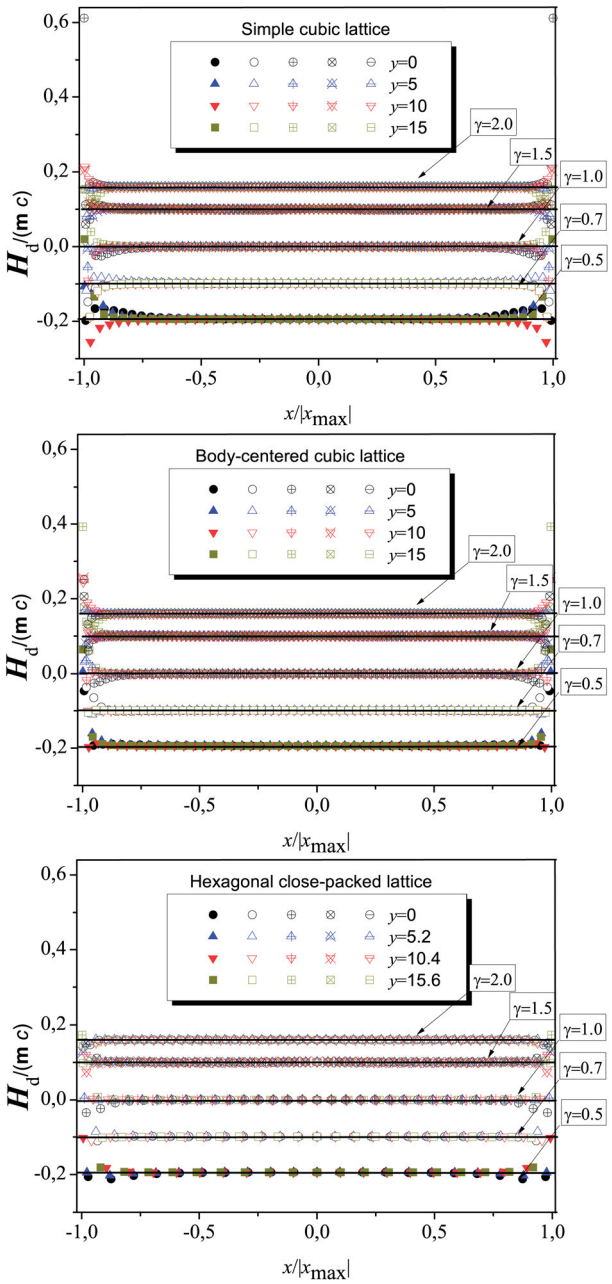

Fig. 3 The normalized dipole magnetic field $H_d/(mc)$ as a function of coordinates x and y, $x_{max} = A\sqrt{1 - y^2/B^2}$. Results are presented for five different values of the aspect ratio γ.

Due to the axial symmetry it is sufficient to consider the distribution of the magnetic field on the xy-plane at $z = 0$. Fig. 3 shows the normalized dipole magnetic field $\mathbf{H}_d/(\mathbf{m}c)$ as a function of a dimensionless $x/|x_{max}|$ coordinate for different values of y at $z = 0$. Here $x \in [-x_{max}, x_{max}]$, where $x_{max} = A\sqrt{1 - y^2/B^2}$. To obtain good statistics we choose the size of the sample such that $AB^2 = (40a)^3$ for all three lattices, where a is the edge of the lattice. Thus, the ellipsoid contains approximately 2.6×10^5, 5.2×10^5 and 3.7×10^5 particles for SC, BCC and HCP lattices, respectively.

The points in Fig. 3 show the exact values of the induced magnetic field as a function of coordinates $\mathbf{r}_j$, calculated using explicit summation over all particles according to eqn (2) and (3). The sum in eqn (3) was performed over sites of the regular lattices. The solid lines in Fig. 3 show the values of $\mathbf{H}_d/(\mathbf{m}c)$ averaged over all points $\mathbf{r}_j$. One can see that the induced magnetic field $\mathbf{H}_d$ is constant and does not depend on the spatial position inside the sample, except some points on the vicinity of the surface. The field on the surface is known to change step-wise.[36,37] Thus, our calculations confirm the result of the continuum-mechanics approach that the magnetic field inside an ellipsoid is constant and has a step-wise peculiarity on the surface.[36,37] It increases with the increase of the sample aspect ratio γ.

Fig. 4 shows the value of $\langle \mathbf{H}_d \rangle/(\mathbf{m}c)$ averaged over all particles as a function of γ using three introduced lattice models for the isotropic particle distribution. The points illustrate the result of exact summation (eqn (2) and (3)) over all particles inside the ellipsoid. The line shows the value $\langle \mathbf{H}_d \rangle$ which is provided by the theoretical formalism given by eqn (2), (4), (5) and (12).

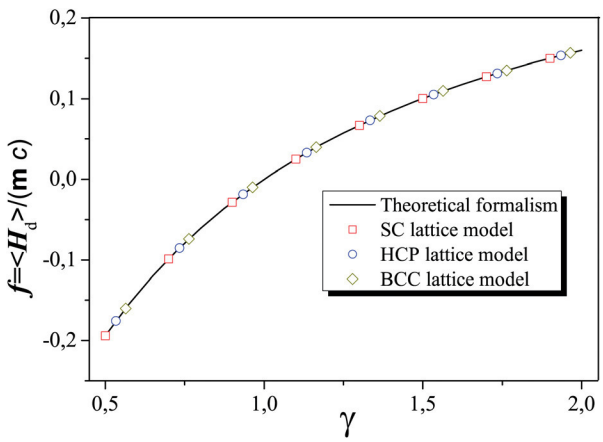

Fig. 4 The normalized dipole magnetic field $\langle \mathbf{H}_d \rangle/(\mathbf{m}c)$, averaged over all particles as a function of γ, calculated for the SC, BCC and HCP lattice particle distributions using the exact summation (points) and the theoretical formalism (line). To avoid the crowding of points on the graph, we calculated $\langle \mathbf{H}_d \rangle/(\mathbf{m}c)$ for different lattice models at slightly different values of γ.

One can see a good agreement between the values f obtained by using explicit summation (points) and using the theoretical formalism (lines). All points in Fig. 4 lie on the same line which is described by factor $f = f_{macro}(\gamma)$, since $f_{micro}(\{\mathbf{r}_{ij}\}) = 0$ for all

lattice models due to symmetrical distributions of particles inside the microsphere.

Thus, starting from a model with the discrete particle distribution, we show that the internal magnetic field does not depend on the particle positions for the isotropic particle distribution. The averaged magnetic field is shown to be well described by the theoretical formalism developed in Section 2.1.

2.3 Anisoptropic particle distribution

Now we consider the anisotropic particle distribution inside the MSEs with different aspect ratios γ. To consider anisotropic particle distributions (chain-like and plane-like distributions) we use the tetragonal lattice model which represents a deformed simple cubic lattice (see Fig. 5).[31] The values $L_x^{(0)}$, $L_y^{(0)}$, $L_z^{(0)}$ ($L_y^{(0)} = L_z^{(0)}$) are the lattice edges. We introduce the anisotropy parameter $\alpha = L_x^{(0)}/L_y^{(0)}$, which defines an anisotropy of spatial distribution of particles along x- and y-axis: if $\alpha = 1$ one has the isotropic particle distribution, if $\alpha < 1$ or $\alpha > 1$ one has the chain-like or plane-like particle distributions, respectively.

Fig. 6 shows the normalized dipole magnetic field $\mathbf{H}_d/(\mathbf{m}c)$ as a function of the dimensionless $x/|x_{max}|$ coordinate inside the prolate MSE sample with $\gamma = 2.0$. The values of $\mathbf{H}_d/(\mathbf{m}c)$ were calculated at $z = 0$ and at different x, y-coordinates for tetragonal lattices with varying values of the anisotropy parameter α. One can see that at each value of α the magnetic field is independent of the spatial position, except the points in the vicinity of the surface where the field changes step-wise.

In Fig. 7 the averaged values of $\langle \mathbf{H}_d \rangle/(\mathbf{m}c)$ as functions of the aspect ratio γ, calculated for the particle distribution on a tetragonal lattice with different anisotropy parameter α, are presented. The symbols mark the values of $\langle \mathbf{H}_d \rangle/(\mathbf{m}c)$ averaged explicitly over all particles in the ellipsoid, calculated using eqn (2) and (3). The solid lines mark results of the theoretical formalism given by eqn (2), (4), (5) and (12). It includes the sum f_{micro} over particles in the microsphere of radius $r_0 \gg R_0$ and the analytical integral f_{macro}. Note that for an anisotropic particle distribution $f_{micro} \neq 0$ if $\alpha \neq 1$, f_{micro} being a function of α. Thus, in contrast to the isotropic particle distribution, the magnetic field in a sample with the anisotropic particle distribution depends on the degree of anisotropy of particle distribution. One can see from Fig. 7 a good agreement between the exact summation over all particles and the theoretical formalism.

Thus, the formalism developed in Section 2.1 allows us to describe in a simple way the magnetic field inside an MSE at the variable shape factor γ and for different particle distributions inside the MSE, the particle distribution being varied in a whole sample. Moreover, one can see that the value of the magnetic field provided by the proposed theoretical formalism is independent of the shape of the surface which splits the factor f into two contributions f_{micro} and f_{macro}. Indeed, the integral from an arbitrary splitting surface $r_1(\theta)$ until the boundary of the sample is presented as a sum of the integrals from $r_1(\theta)$ until r_0 ($r_0 > r_1(\theta)$) and from r_0 until the boundary of the sample. The latter integral equals f_{macro} given by eqn (12) and (13); the former one is well approximated by the sum over the particles at $r_1(\theta) < |\mathbf{r}_{ij}| < r_0$, since $R_0 \ll r_1(\theta)$. The last sum at $r_1(\theta) < |\mathbf{r}_{ij}| < r_0$ together with the sum at $|\mathbf{r}_{ij}| < r_1(\theta)$ equals f_{micro} given by eqn (5). Thus, the magnetic field provided by the proposed theoretical method is independent of the shape of the splitting surface. To check this conclusion, we used the ellipsoidal splitting surfaces of different aspect ratios and obtained the same values of the magnetic field presented by the lines in Fig. 4 and 7.

The idea to split the magnetic field into two contributions f_{micro} and f_{macro} is very similar to the well-known concept of the Lorenz sphere.[38] However, in contrast to the Lorentz–Lorenz approach, in which $f_{micro} = 0$, the factor f_{micro}, as we showed explicitly in Section 2, depends on the particle distribution and can differ from zero. One can see from Fig. 4 and 7 that the proposed theoretical formalism provides a strong enough approximation for the magnetic field inside an MSE with large number of included particles. Below we use this approximation to calculate the magnetization of an MSE.

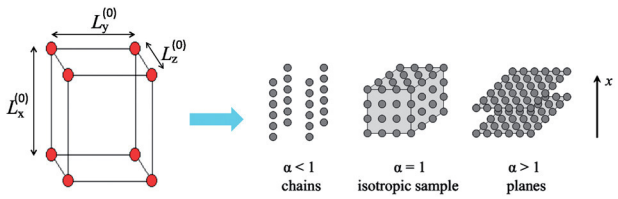

Fig. 5 The cell of the tetragonal lattice, characterized by the structural parameter $\alpha = L_x^{(0)}/L_y^{(0)}$; $L_y^{(0)} = L_z^{(0)}$.

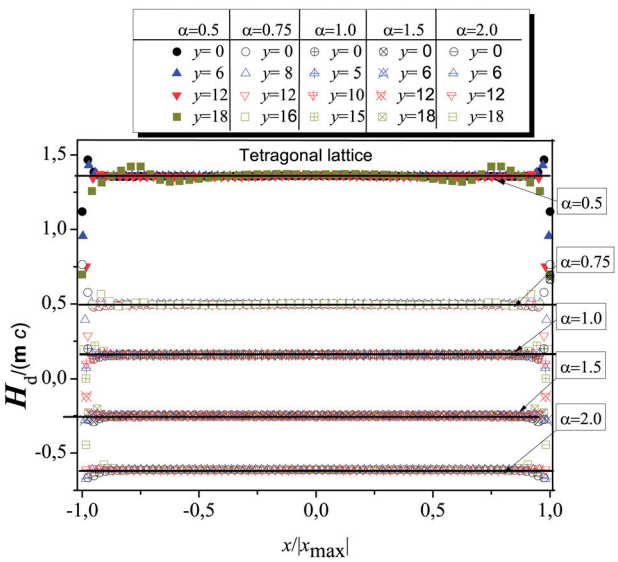

Fig. 6 The normalized dipole magnetic field $H_d/(mc)$ as a function of the dimensionless $x/|x_{max}|$ coordinate in the case of tetragonal lattice distribution of magnetic particles inside the prolate MSE sample with $\gamma = 2.0$. Results are presented for five different values of the lattice anisotropy α.

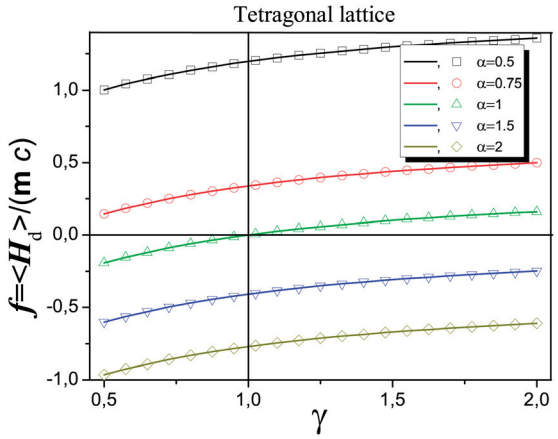

Fig. 7 The normalized dipole magnetic field $\langle H_d \rangle/(mc)$, averaged over all particles as a function of γ, calculated for the tetragonal lattice particle distribution using the exact summation (points) and the theoretical formalism (lines). Results are presented for five different values of the lattice anisotropy α.

3 Magnetization of MSE

Bulk magnetisation is one of the characteristic quantities that is usually measured in experiments. In the previous section we assumed that each magnetic particle has the same magnetic moment $\mathbf{m}$ inside an ellipsoidal MSE under a homogeneous external magnetic field $\mathbf{H}_0$. One can see now that this assumption is a very good approximation for the magnetic moment distribution inside the MSE. Indeed, each magnetic moment $\mathbf{m}_j$ is determined only by the total magnetic field, $\mathbf{H}$, which is induced in the vicinity of a j-th magnetic particle by all external sources: $\mathbf{m}_j = \mathbf{m}_j(\mathbf{H})$. Since the total magnetic field, $\mathbf{H} = \mathbf{H}_0 + \mathbf{H}_d$, is constant inside a sample, the magnetic moments should be also constant: $\mathbf{m}_j = \mathbf{m} = \text{const}$. This consistency fails only in a thin layer close to the surface of the macroscopic sample, where $\mathbf{H}_d$ is not constant.

We estimated the thickness of this layer to be $\sim 10R_0$,[31] where R_0 is the average distance between neighbouring particles. Therefore, one can neglect the contribution from this layer to the total magnetization and the magnetic energy, if the characteristic size of a sample A is much higher than $10R_0$: $A \gg 10R_0$. The last condition puts a restriction on the volume fraction of particles ϕ as follows: $\phi \sim (R/R_0)^3 \gg (10\,R/A)^3$. If we take a typical size of particles $R \sim 1$ μm as well as $A \sim 1$ cm then $\phi \gg 10^{-9}$, the condition which is always fulfilled. Thus, in a very good approximation the magnetic moments and the magnetic field are supposed to be constant inside an MSE.

It is known from classical studies that the magnetic dipole $\mathbf{m}$ of a spherical particle, placed into the external magnetic field $\mathbf{H}$, can be calculated for linear magnetics as[37]

$$\mathbf{m} = \nu \frac{3\chi}{(3+\chi)} \mathbf{H}, \tag{14}$$

where ν is the volume of the particle. As we mentioned above, $\mathbf{H}$ consists of two contributions:

$$\mathbf{H} = \mathbf{H}_0 + \mathbf{H}_d, \tag{15}$$

where the value $\mathbf{H}_d$ is also a function of $\mathbf{m}$ according to eqn (2). In other words, eqn (2), (14) and (15) represent the condition of self-consistency for the magnetic moment $\mathbf{m}$. Thus, the value $\mathbf{m}$ is to be found from the following equation:

$$\mathbf{m} = \nu \frac{3\chi}{(3+\chi)} (\mathbf{H}_0 + \mathbf{m}cf). \tag{16}$$

From the last equation we obtain an expression for the magnetic dipole as

$$\mathbf{m} = \frac{\nu \mathbf{H}_0}{\chi^{-1} + \frac{1}{3} - \phi f}, \tag{17}$$

where $\phi = \nu c$ is the volume fraction of the magnetic particles.

Now, the bulk magnetization $\mathbf{M}_V$ reads

$$\mathbf{M}_V = \mathbf{m}c \tag{18}$$

that finely gives

$$\mathbf{M}_V = \frac{\phi \mathbf{H}_0}{\chi^{-1} + \frac{1}{3} - \phi f}. \tag{19}$$

Here we note that the last equation follows from eqn (14) which is valid only for linear magnetics. For nonlinear magnetics the relationship between $\mathbf{M}_V$ and ϕ can be more complicated as compared with eqn (19). Moreover, for high values of ϕ the approximation of point-like dipoles fails and, thus, the finite size of magnetic particles can play a significant role. However, one can expect that the approach presented above provides a good approximation in the region, $\phi \leq 0.2$ where the Lorentz–Lorenz approach is valid,[38] since it uses also the point-like approximation for dipole–dipole interactions.

From eqn (19) one can obtain a very important result that the magnetization $\mathbf{M}_V$ is the monotonically increasing function of ϕ, γ and χ at fixed particle distribution, since

$$\frac{\partial \mathbf{M}_V}{\partial \phi} = \mathbf{H}_0 \frac{\chi^{-1} + \frac{1}{3}}{\left(\chi^{-1} + \frac{1}{3} - \phi f\right)^2} > 0, \tag{20}$$

$$\frac{\partial \mathbf{M}_V}{\partial \gamma} = \mathbf{H}_0 \frac{\phi^2}{\left(\chi^{-1} + \frac{1}{3} - \phi f\right)^2} \frac{\partial f_{\text{macro}}}{\partial \gamma} > 0, \tag{21}$$

and

$$\frac{\partial \mathbf{M}_V}{\partial \chi} = \mathbf{H}_0 \frac{\phi}{\chi^2 \left(\chi^{-1} + \frac{1}{3} - \phi f\right)^2} > 0. \tag{22}$$

Here we have used that $\partial f_{\text{micro}}/\partial \gamma = 0$. These tendencies are illustrated in Fig. 8, where the ratio $\mathbf{M}_V/\mathbf{H}_0$ is presented as a function of ϕ for different values of γ (Fig. 8a) and for different values of α (Fig. 8b). Thus, starting from a general model with the discrete particle distribution we obtained general results for the dependence of $\mathbf{M}_V$ on the parameters ϕ, χ, γ and α.

In previous sections the parameters γ and α were varied independently. Certainly, there should exist some coupling of these parameters. In the next section we introduce different approaches for this coupling and analyse the free energy in order to study the mechanical response of the MSEs.

4 Free energy and elastic response

4.1 General equations

Interaction between the induced magnetic moments leads to pair-wise attraction and repulsion of the magnetic particles depending on their mutual positions.[31,32] This behaviour of the particles leads to elastic response of the sample. Thus, an ellipsoidal sample can change its shape under a magnetic field. Let the semi-axes of an ellipsoidal sample be changed from the initial values A_0, $B_0 = C_0$ to the new values A, $B = C$. The initial aspect ratio $\gamma_0 = A_0/B_0$ is considered as a parameter, which characterizes the initial shape of the sample. The incompressibility of the sample provides the expressions for the semi-axes of the ellipsoid:

$$A = A_0(1 + \varepsilon), \quad B = C = \frac{B_0}{\sqrt{1+\varepsilon}}, \tag{23}$$

where ε is the relative elongation (strain) of the sample. Then, parameters γ, γ_0 and ε are related *via* the expression

$$\gamma = \gamma_0(1 + \varepsilon)^{3/2}. \tag{24}$$

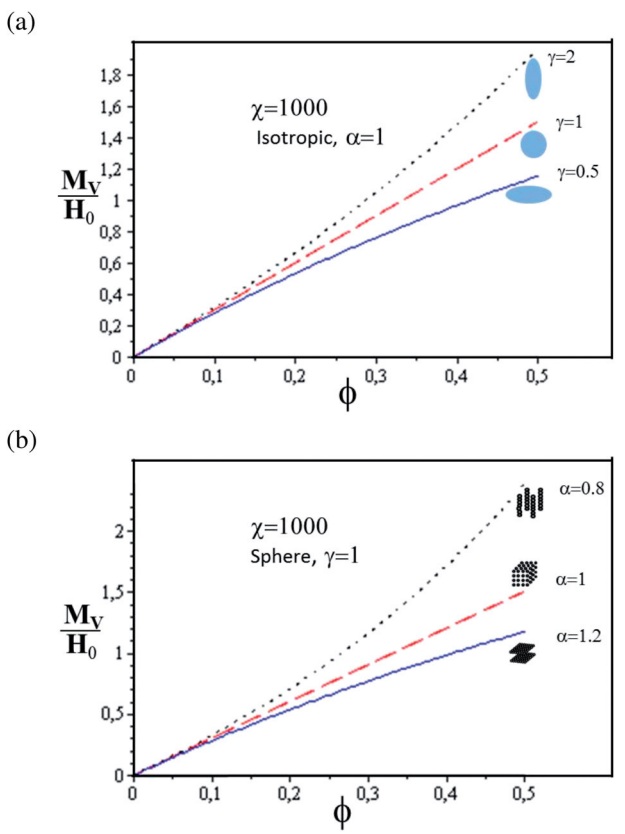

Fig. 8 The ratio M_V/H_0 as a function of ϕ at fixed values of χ and α (a) and at fixed values of χ and γ (b).

In the absence of other mechanical loading on the MSE, the sample tends to achieve the equilibrium state, which is characterized by the equilibrium elongation ε_{eq}. The equilibrium elongation ε_{eq} of the sample is determined from the minimum of the free energy of the MSE with respect to ε at the constant value of external magnetic field $\mathbf{H}_0$:

$$\left.\frac{\partial F}{\partial \varepsilon}\right|_{\mathbf{H}_0=\text{const}} = 0. \tag{25}$$

Here F is the free energy per unit volume. Further, one can calculate the elastic modulus E as the second derivative of the free energy with respect to ε:

$$E = \left.\frac{\partial^2 F}{\partial \varepsilon^2}\right|_{\varepsilon=\varepsilon_{eq}}. \tag{26}$$

Here we consider such a geometry of tensile deformation, when the mechanical force is applied along the external magnetic field $\mathbf{H}_0$, *i.e.* along the x-axis. The free energy of the MSE consists of two parts:[31,32]

$$F = F_{elast} + F_{magn}, \tag{27}$$

where F_{elast} is the elastic free energy that arises from the entropic elasticity of polymer chains, and F_{magn} is the magnetic free energy. In the case of small linear deformation of an incompressible MSE, the elastic free energy per unit volume can be expressed through the Hooke law:[39]

$$F_{elast} = \frac{E_0\varepsilon^2}{2}, \tag{28}$$

where the material parameter E_0 is the elastic modulus of a filled polymer matrix. Here we assume that the value of E_0 includes contributions of different possible effects into the elastic energy appearing under elongation of a sample. Among these effects are the hydrodynamic reinforcement of an elastic matrix by the hard particles at different concentrations,[40,41] the reinforcement due to appearance of glass-like layers formed by the polymer chains that are localized on surfaces of active particles[42] as well as the contribution from deforming interphase domains in the composite.[42] However, we do not discuss here the dependence of E_0 on these effects, since this task is a special problem in the theory of elasticity for isotropic reinforced rubbers.[42] Instead, in our theory we use E_0 as a phenomenological parameter which can be extracted from experimental mechanical data of an MSE in the absence of the magnetic field.

The magnetic free energy F_{magn} for linear magnetics is given by the following equation:[35]

$$F_{magn} = -\frac{1}{2}\mu_0 \mathbf{M}_V \mathbf{H}_0, \tag{29}$$

where $\mathbf{M}_V$ is the magnetization of the sample according to eqn (18) and (19), and $\mu_0 = 4\pi \times 10^{-7}$ N A^{-2} is the permeability of vacuum. Substituting eqn (19) into (29) we get

$$F_{magn} = -\frac{1}{2}\mu_0 \frac{\phi \mathbf{H}_0^2}{\chi^{-1} + \frac{1}{3} - \phi f}. \tag{30}$$

Note that $f = f_{\text{micro}}(\{\mathbf{r}_{ij}\}) + f_{\text{macro}}(\gamma)$. Thus, the mechanical properties of MSE are determined by the particle distribution $\{\mathbf{r}_{ij}\}$ as well as by the initial shape of the sample γ_0.

Using eqn (25), (27), (28) and (30), one can obtain the equilibrium elongation ε_{eq}. Expanding into the Taylor series and keeping the main term with respect to H_0 we get ε_{eq} for the linear-response regime in the following form:

$$\varepsilon_{\text{eq}} = K_\varepsilon \frac{\mu_0 \mathbf{H}_0{}^2}{2E_0}, \tag{31}$$

where the numerical coefficient K_ε is given by

$$K_\varepsilon = \left. \frac{\phi^2 \frac{\partial f}{\partial \varepsilon}}{\left(\chi^{-1} + \frac{1}{3} - \phi f\right)^2} \right|_{\varepsilon=0}. \tag{32}$$

One can see from eqn (31) that the equilibrium elongation ε_{eq} is a quadratic function of the external magnetic field $\mathbf{H}_0$ in the linear-response regime. The sign (contraction or expansion) and magnitude of ε_{eq} are determined by the sign and magnitude of the parameter K_ε.

Using eqn (26)–(28) and (30), one can calculate the change of the elastic modulus, $\Delta E = E - E_0$ (*i.e.* the magneto-rheological effect), for the linear-response regime in the following form:

$$\Delta E = K_E \frac{\mu_0}{2} \mathbf{H}_0{}^2. \tag{33}$$

The coefficient K_E is determined by the first non-zero term in the Taylor expansion and is given by

$$K_E = \left. \frac{\phi^2}{\left(\chi^{-1} + \frac{1}{3} - \phi f\right)^2} \left(-\frac{\partial^2 f}{\partial \varepsilon^2} - \frac{2\phi \left(\frac{\partial f}{\partial \varepsilon}\right)^2}{\chi^{-1} + \frac{1}{3} - \phi f} \right) \right|_{\varepsilon=0}. \tag{34}$$

Note that both coefficients K_ε and K_E depend not only on the initial shape of the MSE sample γ_0, volume fraction ϕ and initial particle distribution $\{\mathbf{r}_{ij}\}$ but also on the coupling between the particle distribution $\{\mathbf{r}_{ij}\}$ and elongation ε due to the term $\frac{\partial f}{\partial \varepsilon}$. Below we consider two different approximations for the coupling between $\{\mathbf{r}_{ij}\}$ and ε.

4.2 Absence of elastic coupling between sample elongation and position of particles

In this section we consider the mechanical response of the MSEs in the absence of elastic coupling between the particle distribution $\{\mathbf{r}_{ij}\}$ and the elongation ratio ε: $\frac{\partial \{\mathbf{r}_{ij}\}}{\partial \varepsilon} = 0$. This situation corresponds to slightly cross-linked MSEs, in which the particles can freely move inside the polymer matrix, keeping an initial spatial distribution at the variation of ε. In this case the values of K_ε and K_E are determined by the shape-factor f_{macro} and its derivatives as well as by the initial local particle distribution through the factor f_{micro}, but not by its derivatives, since $\frac{\partial f_{\text{micro}}}{\partial \varepsilon} = 0$ and $\frac{\partial^2 f_{\text{micro}}}{\partial \varepsilon^2} = 0$. The initial particle distribution can be either isotropic or anisotropic (see Section 2.2) that corresponds to $f_{\text{micro}}(\{\mathbf{r}_{ij}\}) = 0$ or $f_{\text{micro}}(\{\mathbf{r}_{ij}\}) \neq 0$, respectively. Below, we consider these two cases in detail.

Isotropic particle distribution. In Fig. 9 the coefficients K_ε and K_E are presented as a function of γ_0 for the isotropic particle distribution (represented by the SC lattice model, $\alpha = 1$) for different values of ϕ. One can see that the coefficient K_ε is always positive and thus $\varepsilon_{\text{eq}} > 0$ as predicted by the continuum-mechanics approach.

The coefficient K_E varies the sign with increasing γ_0. It is negative for strongly oblate ellipsoids. As one can see from Fig. 9 the coefficient K_ε has a maximum in the vicinity $\gamma_0 = 1$, whereas the coefficient K_E has a maximum which shifts with the increase of ϕ from $\gamma_0 \approx 1$ to $\gamma_0 \approx 3$. Both coefficients K_ε and K_E increase with increasing ϕ at a fixed value of γ_0, showing that the magnetostriction and the magneto-rheological effect increase with increase of ϕ.

Anisotropic particle distribution. In Fig. 10 the coefficients K_ε and K_E are presented as a function of γ_0 for the chain-like ($\alpha = 0.8$), isotropic ($\alpha = 1.0$) and plane-like ($\alpha = 1.2$) structures at $\phi = 0.3$ and $\chi \gg 1$. One can see that the coefficient K_ε is positive for all values of α and thus $\varepsilon_{\text{eq}} > 0$. K_ε has a maximum in the vicinity of $\gamma_0 = 1$, but for the chain-like structure this maximum is shifted to larger γ_0.

The coefficient K_E varies the sign with increasing γ_0 similar to the case of isotropic particle distribution. It is negative for strongly oblate ellipsoids and has a maximum at $\gamma_0 \approx 2.5$. The main result is that the anisotropy of the particle distribution strongly affects the magneto-rheological effect ΔE: it is much more pronounced for the chain-like structure with $\alpha = 0.8$ in comparison with the isotropic ($\alpha = 1.0$) and plane-like ($\alpha = 1.2$) structures.

We note that similar qualitative behaviour of the equilibrium elongation ε_{eq} and magneto-rheological effect ΔE (not shown here) takes place for other lattice models (BCC and HCP lattices) that can be used for describing the initial particle distribution within a MSE sample. Since the sign of K_ε and K_E is determined only by the derivatives $\frac{\partial f_{\text{macro}}}{\partial \varepsilon}$ $\left(\text{as } \frac{\partial f_{\text{micro}}}{\partial \varepsilon} = 0\right)$, the use of another lattice model does not change the signs of ε_{eq} and ΔE but provides only small quantitative changes in these quantities.

Importantly, our general results presented above can reproduce the findings of the continuum-mechanics approach for a spherical sample ($\gamma_0 = 1$) with the isotropic particle distribution ($\alpha = 1$).[24] Estimation of $K_\varepsilon(\gamma_0)$ at $\gamma_0 = 1$ gives 2/5. Thus, for spherical samples we get a result that coincides with prediction of the continuum-mechanics approach:[24]

$$\varepsilon_{\text{eq}} = \frac{\mu_0 \mathbf{M}_V{}^2}{5E_0}. \tag{35}$$

We see that ε_{eq} in eqn (35) is always positive, being an even function of magnetization $\mathbf{M}_V$. It increases at increasing magnetization (*i.e.* at increasing magnitude of the internal magnetic field $\mathbf{H}_0$) for the uniformly magnetized elastic sphere. Estimation of K_E at $\gamma_0 = 1$ gives 4/7 that provides the following result:

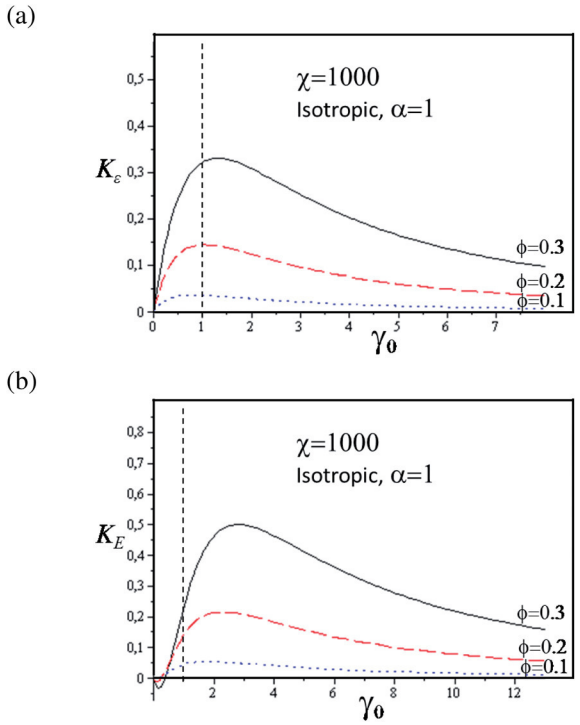

Fig. 9 The coefficients K_ε (a) and K_E (b) as a function of the initial shape γ_0, calculated in the case of isotropic particle distribution for different values of ϕ and at $\chi = 1000$.

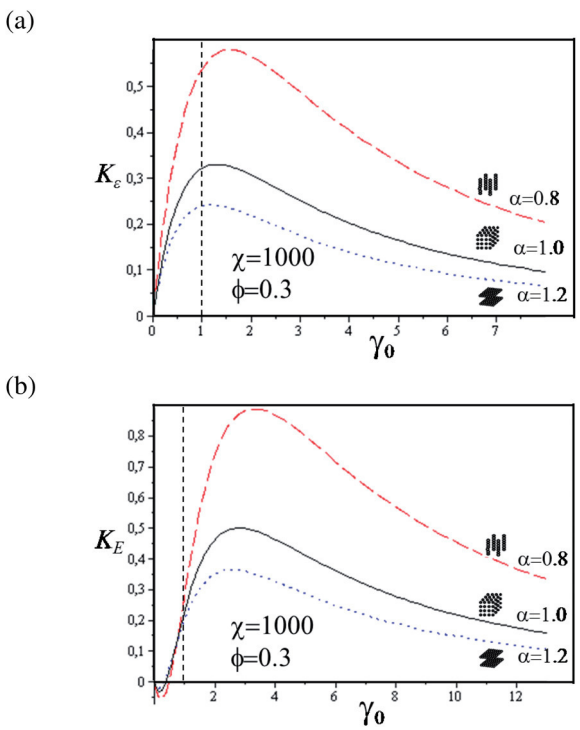

Fig. 10 The coefficients K_ε (a) and K_E (b) as a function of the initial shape γ_0, calculated for the chain-like ($\alpha = 0.8$), isotropic ($\alpha = 1.0$) and plane-like ($\alpha = 1.2$) structures at $\phi = 0.3$ and $\chi = 1000$.

$$\Delta E = \frac{2}{7}\mu_0 \mathbf{M} \nu^2. \tag{36}$$

To our knowledge, the value ΔE was not yet calculated in the framework of the continuum-mechanics approach. Thus, this result is obtained for the first time in the present study.

To summarize, the initial shape of the MSE sample γ_0, volume fraction ϕ and an initial particle distribution $\{\mathbf{r}_{ij}\}$ strongly affect the equilibrium elongation ε_{eq} and the magneto-rheological effect ΔE even in the absence of elastic coupling between $\{\mathbf{r}_{ij}\}$ and ε.

4.3 Strong affine coupling between sample elongation and position of particles

Now we will consider the mechanical response of MSEs in the presence of strong elastic coupling between the particle distribution $\{\mathbf{r}_{ij}\}$ and the elongation ratio ε. This means that $\frac{\partial f_{micro}}{\partial \varepsilon} \neq 0$ and $\frac{\partial^2 f_{micro}}{\partial \varepsilon^2} \neq 0$. This situation corresponds to highly cross-linked MSEs, in which the particles cannot freely move inside the polymer matrix but rather move affinely with it. In this case the values of K_ε and K_E are determined both by the shape-factor f_{macro} and by the factor f_{micro} which depends on the local rearrangement of particle distribution $\{\mathbf{r}_{ij}\}$ inside the microsphere. As in our previous works,[31,32] we assume the affine deformation and incompressibility of the sample. This allows us to calculate new positions of the particles:

$$\begin{aligned}(\mathbf{r}_{ij})_x &= (\mathbf{r}^0_{ij})_x(1+\varepsilon),\\ (\mathbf{r}_{ij})_y &= (\mathbf{r}^0_{ij})_y(1+\varepsilon)^{-1/2},\\ (\mathbf{r}_{ij})_z &= (\mathbf{r}^0_{ij})_z(1+\varepsilon)^{-1/2},\end{aligned} \tag{37}$$

where $\mathbf{r}^0_{ij}$ are the vectors connecting i-th and j-th particles in the absence of the magnetic field.

Note that after application of the external magnetic field and deformation of the MSE, the function f_{micro} and its derivatives should be calculated in the microsphere with a constant radius r_0. We calculate the values of K_ε and K_E using eqn (32) and (34). In contrast to Section 4.2, here we take into account that the factor f_{micro} is a function of ε according to eqn (5) and (37).

Isotropic particle distribution. In Fig. 11 the coefficient K_ε is presented as a function of γ_0 for the isotropic particle distribution (represented by three different lattice models) at different ϕ and $\chi \gg 1$.

One can see that the behaviour of the coefficient K_ε shows a strong dependence on the initial particle distribution due to the elastic coupling between particle distribution $\{\mathbf{r}_{ij}\}$ and elongation ratio ε in the microsphere. The SC and HCP lattice models provide the negative coefficient K_ε, whereas the BCC lattice model gives the positive value of K_ε. From eqn (32) it can be seen that the sign of K_ε is determined from the competition between $\frac{\partial f_{micro}}{\partial \varepsilon}$ and $\frac{\partial f_{macro}}{\partial \varepsilon}$. As shown in Section 4.2, the contribution from $\frac{\partial f_{macro}}{\partial \varepsilon}$ is always positive. In the SC lattice model the

contribution from $\frac{\partial f_{micro}}{\partial \varepsilon}$ is found to be negative and exceeding a contribution from the shape factor. In the HCP lattice model we see that both contributions have the opposite sign, but the contribution from $\frac{\partial f_{micro}}{\partial \varepsilon}$ exceeds the contribution from $\frac{\partial f_{macro}}{\partial \varepsilon}$. In the BCC lattice model both contributions have the same sign and provide a positive value of K_ε. In all three lattice models the increase of the volume fraction of particles ϕ provides the increase in the magnitude of K_ε.

It is interesting to compare the results given in Fig. 11a–c for different lattices with the magneto-induced deformation ε_{eq} of MSEs with random (gas-like) distribution of particles.[43,44] The studies in ref. 43 and 44 demonstrated that for random distribution of particles the value of ε_{eq} can change its sign with increasing γ_0: it is negative at $\gamma_0 \ll 1$ or $\gamma_0 \gg 1$ and it is positive at intermediate values of γ_0. One can see from Fig. 11 that for the BCC lattice ε_{eq} is positive and has a maximum, whereas it is negative for the SC and HCP lattices. Thus, for a random distribution (after averaging "over all lattices") one can expect qualitatively a non-monotonic dependence of magneto-induced deformation on the parameter γ_0 similar to that given in ref. 43 and 44. Application of the random distribution to our formalism is a special task which can be solved in the nearest future.

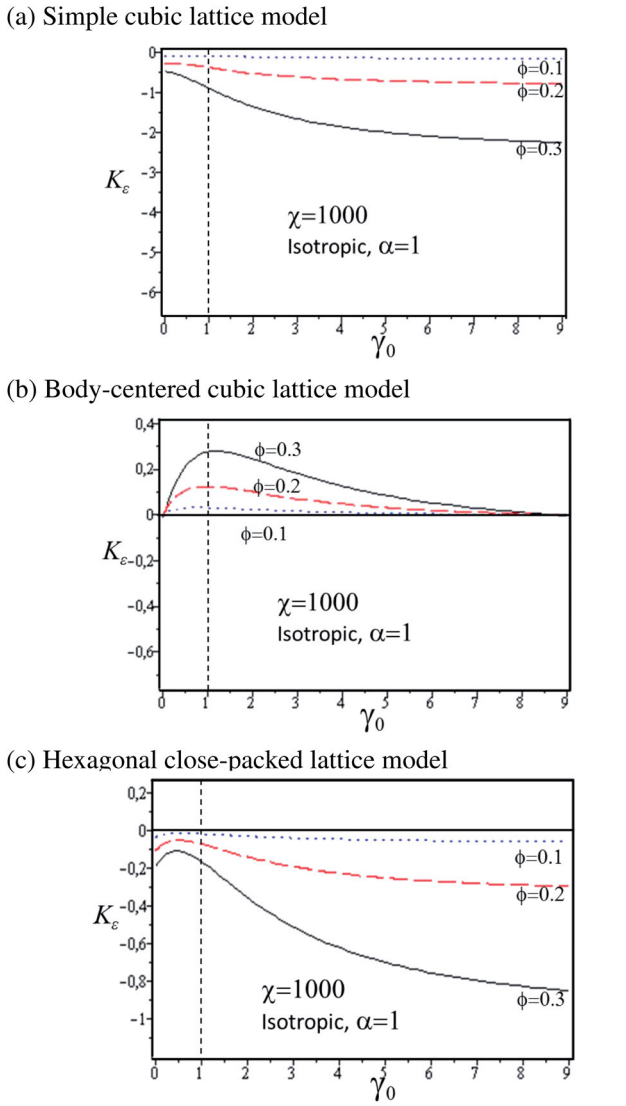

Fig. 11 The coefficient K_ε as a function of the initial shape γ_0, calculated in the case of isotropic particle distribution at different values of ϕ and at $\chi = 1000$.

In Fig. 12 the coefficient K_E is presented as a function of γ_0 in the case of isotropic particle distribution (represented by three different lattice models) for different ϕ and $\chi \gg 1$. Fig. 12 shows a strong dependence of the coefficient K_E on the initial particle distribution. In the case of the strong elastic coupling between particle distribution $\{\mathbf{r}_{ij}\}$ and elongation ratio ε, only the HCP lattice model predicts the positive values of K_E, while both the SC and BCC lattice models provide the negative magneto-rheological effect. In all three lattice models the increase of the volume fraction of particles ϕ provides the increase of the magnitude of K_E.

Anisotropic particle distribution. Fig. 13 and 14 present the coefficients K_ε and K_E as functions of γ_0 for the chain-like ($\alpha = 0.8$), isotropic ($\alpha = 1.0$) and plane-like ($\alpha = 1.2$) structures at volume fraction $\phi = 0.3$ and magnetic susceptibility $\chi \gg 1$.

One can see that the magnetostriction and magneto-rheological effect are negative in the case of the SC lattice model for chain-like, isotropic and plane-like structures. In the case of the BCC lattice model, the values of K_ε and K_E vary their sign: for the chain-like structures both coefficients are negative, that is, similar to the case of the SC lattice model. For the isotropic distribution K_ε is positive, while K_E is slightly negative. For the plane-like structures both K_ε and K_E are positive. It reflects a non-trivial competition between contributions of the factors $\frac{\partial f_{micro}}{\partial \varepsilon}$ and $\frac{\partial f_{macro}}{\partial \varepsilon}$ as well as $\frac{\partial^2 f_{micro}}{\partial \varepsilon^2}$ and $\frac{\partial^2 f_{macro}}{\partial \varepsilon^2}$ in eqn (34). In the HCP lattice model, K_ε also changes the sign with α, whereas K_E is always positive. We can conclude that the presence of affine coupling between the particle distribution $\{\mathbf{r}_{ij}\}$ and elongation ratio ε strongly affects the mechanical behaviour of the MSE under a homogeneous magnetic field.

Interestingly, for chain-like structures ($\alpha \approx 0.9$) a non-monotonic dependence of ε_{eq} on γ_0 is observed similar to ref. 43 and 44: $\varepsilon_{eq} < 0$ at $\gamma_0 \ll 1$ or $\gamma_0 \gg 1$ and $\varepsilon_{eq} > 0$ at intermediate values of γ_0. Moreover, it was shown in ref. 44 that MSEs, which include short chains formed by particles, expand along the magnetic field. This effect is caused by a change of mutual disposition of short chains.[44] However for MSEs consisting of long chains, which can percolate the sample, the mutual disposition of chains does not play a major role and the magneto-deformation is determined by a reduction of gaps between the neighboring particles.[44] In our model the disposition of neighboring particles inside the chain-like structures is explicitly taken into account. This effect leads either to contraction or to elongation of MSE along the magnetic field, the degree of deformation being a complicated function both of the particle distribution and of the sample aspect ratio γ_0, see Fig. 13. Thus, our theory demonstrates a much richer magneto-mechanical behavior of MSEs depending on the spatial

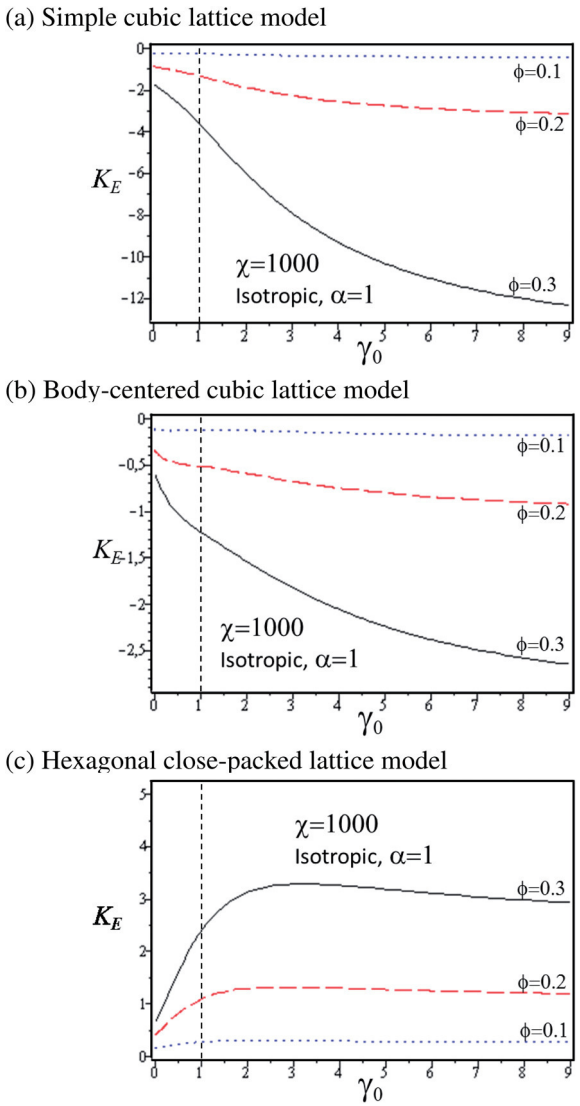

Fig. 12 The coefficient K_E as a function of the initial shape γ_0, calculated in the case of isotropic particle distribution at different values of ϕ and at $\chi = 1000$.

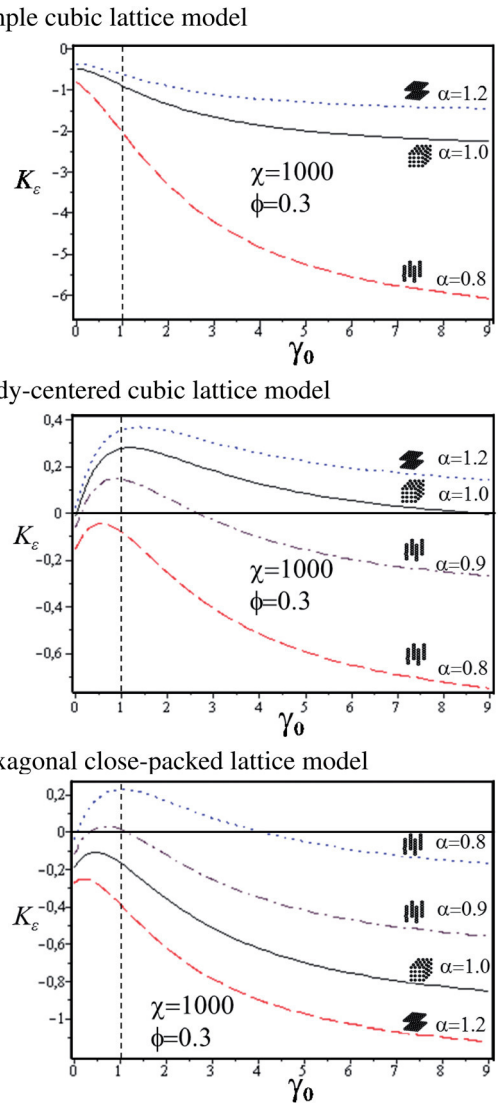

Fig. 13 The coefficient K_ε as a function of the initial shape γ_0, calculated for the chain-like ($\alpha = 0.8$), isotropic ($\alpha = 1.0$) and plane-like ($\alpha = 1.2$) structures at $\phi = 0.3$ and $\chi = 1000$ for three different lattice models.

distribution of magnetic particles as compared to previous studies.[43,44]

5 Discussion

To show the strength of a new theoretical formalism, we considered in this study two limiting cases of the coupling between the particle distribution $\{\mathbf{r}_{ij}\}$ and the elongation ratio ε: (i) no coupling (see Section 4.2), when the particles can freely move inside a matrix keeping an initial spatial distribution at sample deformation and (ii) strong affine coupling (see Section 4.3), when the particles are strictly fixed within the polymer matrix and move affinely with it.

The absence of the elastic coupling between $\{\mathbf{r}_{ij}\}$ and ε provides qualitative predictions that are in good agreement with experiments for MSEs with the isotropic particle distributions. The equilibrium elongation ε_{eq} (ref. 4 and 5) and the magneto-rheological effect ΔE (ref. 8–11) have been shown to be positive and to increase with increase of the magnetic field $\mathbf{H}_0$. Only strongly oblate samples ($\gamma_0 < 0.5$) such as thin disks and shims exhibit the decrease of elastic modulus with increase of the external magnetic field. Further, in agreement with experiments[1] the change of elastic modulus is higher for the chain-like structures as compared with the isotropic particle distributions. However, the absence of the elastic coupling predicts elongation of MSEs with chain-like structures which is in contradiction with a number of experiments.[4,6,7]

The presence of the strong affine coupling between $\{\mathbf{r}_{ij}\}$ and ε provides a much richer behaviour for different lattice models that we used to mimic diverse particle distributions inside the MSE. We found that ε_{eq} and ΔE can be both positive and negative, depending on the initial particle distribution. Thus, assumption of the affine deformation strongly affects the

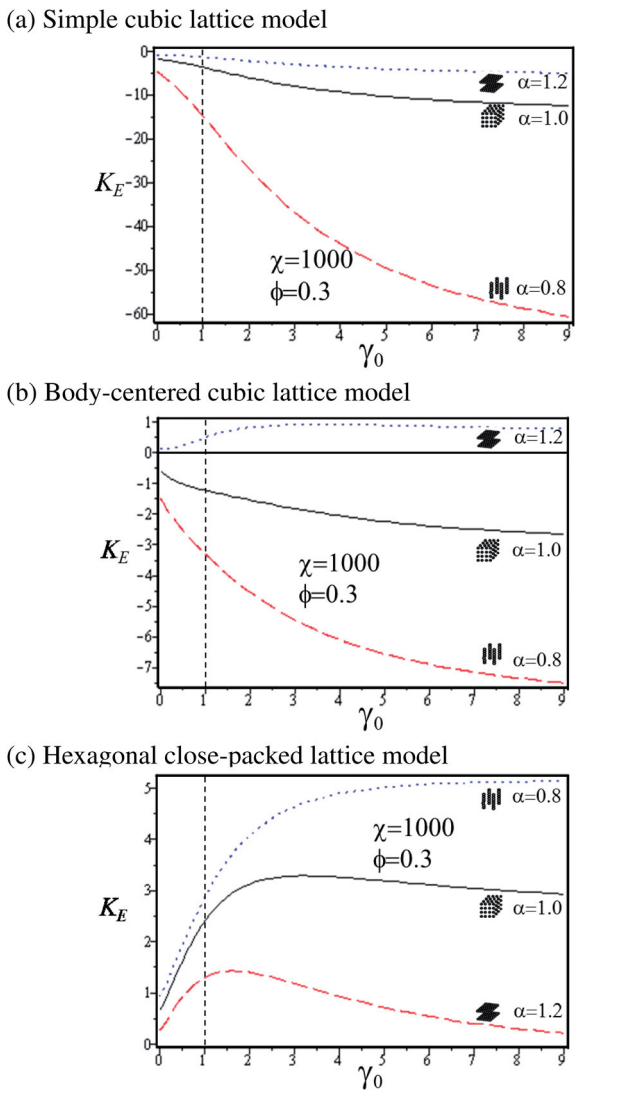

Fig. 14 The coefficient K_E as a function of the initial shape γ_0, calculated for the chain-like ($\alpha = 0.8$), isotropic ($\alpha = 1.0$) and plane-like ($\alpha = 1.2$) structures at $\phi = 0.3$ and $\chi = 1000$ for three different lattice models.

results for the sign of magnetostriction (contraction, expansion) and magneto-rheological effect (softening, stiffening). The presence of affine coupling predicts contraction of a sample for MSEs with the chain-like particle distributions in agreement with experiments.[4,6,7]

In all the cases considered we have neglected a possible rearrangement of particles under a uniform magnetic field in the deforming sample. In particular, we used the assumption of affine deformation, the physical meaning of which is that the particles are rigidly attached to a polymer matrix. The use of such an affine approach is valid for the case of small deformations, *i.e.*, at small external fields or highly cross-linked matrices. The assumption is, however, not valid anymore for MSEs prepared on the basis of soft polymer matrices, in which the flexibility of polymer sub-chains between cross-links allows a considerable degree of particle movement and even diffusion under strong magnetic fields. Indeed, a noticeable rearrangement of particles into chain-like structures was observed recently in MSEs with initially isotropically distributed magnetic particles under application of the magnetic field.[45,46] The authors have explained this effect by the use of a relatively soft polymer matrix which does not restrict alignment of particles into the chains caused by the dipole–dipole interactions between the particles. Also, recent constitutive modelling[22] as well as the wavy particle-chain model[30] shows an importance of consideration of the particle alignment under the magnetic field for description of the mechanical behaviour of MSEs. This means that elastic coupling in the samples with relatively soft polymer matrices is far from being affine.

Note that such a type of non-affine coupling can be taken into account in the frame of our theoretical formalism if we assume that the structure parameter α is a function of the magnetic field $\mathbf{H}_0$. The form of this function is presently unknown and can be established by a careful comparison of theoretical predictions based on different test functions with existing experimental data[45,46] or from appropriate finite element simulations of MSEs. Nevertheless, some predictions can already be made in the frame of the proposed formalism, since it allows us to separate the macroscopic shape effects from the local changes in particle distribution. For example, we may utilize the results presented in Section 4.2 for particle distributions with different anisotropy α. Especially, it is clearly seen from Fig. 10 that at the same volume fraction of the magnetic particles both the magnetostriction and the magneto-rheological effects become much more pronounced, when the particle distribution changes from an isotropic one to the chain-like distribution. If we assume that such a rearrangement of particles is caused by the applied magnetic field, we should expect a considerable increase of magneto-induced deformation and elastic moduli which agrees well with experimental observations.[45,46]

6 Conclusions

In this paper we proposed a new theoretical formalism for the mechanical properties of MSEs which unifies two approaches: the macroscopic continuum-mechanics and microscopic approaches. We have shown that starting from a model with explicit discrete particle distribution one can separate the magnetic field inside the MSE into two contributions: one which depends on the shape of the sample and the other, which depends on the local particle distribution. The behaviour of magneto-induced deformation and elastic modulus as functions of the magnetic field is determined by a non-trivial interplay between the macroscopic and microscopic contributions. Switching off one of these contributions results in a pure microscopic approach[31,32] or in a pure macroscopic approach.[24]

The proposed formalism allows us to perform separation into the macroscopic and microscopic contributions both for the isotropic and for the anisotropic particle distributions. Thus, it can be used to investigate the mechanical properties of MSEs for a wide variety of particle distributions, as well as for a wide variety of sample shapes. The open question at the moment is the strength of elastic coupling between particle

displacements under a uniform magnetic field and the sample deformation. In this study we considered two limiting cases: absence of the coupling and affine coupling. We presume however that the nature of coupling in real samples should lie somewhere between these two limiting cases. Its description needs an additional consideration.

We hope that the theoretical formalism developed in the present study will be useful for further development of this very important class of smart materials. The further step of our studies in this topic will be to find the law of the coupling between local particle movements and the macroscopic deformation and studying its influence on the mechanic properties of MSEs with soft polymer matrices.

Acknowledgements

The financial support of the DFG grant GR 3725/6-1 is gratefully acknowledged.

References

1 G. Filipcsei, I. Csetneki, A. Szilágyi and M. Zrínyi, *Adv. Polym. Sci.*, 2007, **206**, 137–189.
2 S. Abramchuk, E. Kramarenko, D. Grishin, G. Stepanov, L. V. Nikitin, G. Filipcsei, A. R. Khokhlov and M. Zrínyi, *Polym. Adv. Technol.*, 2007, **18**, 513–518.
3 X. Zhang, S. Peng, W. Wen and W. Li, *Smart Mater. Struct.*, 2008, **17**, 045001.
4 G. Y. Zhou and Z. Y. Jiang, *Smart Mater. Struct.*, 2004, **13**, 309–316.
5 G. Diguet, E. Beaugnon and J. Y. Cavaillé, *J. Magn. Magn. Mater.*, 2010, **322**, 3337–3341.
6 M. R. Jolly, J. D. Carlson, B. C. Muñoz and T. A. Bullions, *J. Intell. Mater. Syst. Struct.*, 1996, **7**, 613–622.
7 E. Coquelle and G. Bossis, *J. Adv. Sci.*, 2005, **17**, 132–138.
8 C. Bellan and G. Bossis, *Int. J. Mod. Phys. B*, 2002, **16**, 2447–2453.
9 Z. Varga, G. Filipcsei and M. Zrínyi, *Polymer*, 2006, **47**, 227–233.
10 S. Abramchuk, E. Kramarenko, G. Stepanov, L. V. Nikitin, G. Filipcsei, A. R. Khokhlov and M. Zrínyi, *Polym. Adv. Technol.*, 2007, **18**, 883–890.
11 D. Y. Borin, G. V. Stepanov and S. Odenbach, *J. Phys.: Conf. Ser.*, 2013, **412**, 012040.
12 T. Shiga, A. Okada and T. Kurauchi, *J. Appl. Polym. Sci.*, 1995, **58**, 787–792.
13 S. A. Demchuk and V. A. Kuzmin, *J. Eng. Phys. Thermophys.*, 2002, **75**, 396–400.
14 M. Lokander and B. Stenberg, *Polym. Test.*, 2003, **22**, 245–251.
15 H. X. Deng and X. L. Gong, *J. Intell. Mater. Syst. Struct.*, 2007, **18**, 1205.
16 W.-Q. Jiang, J.-J. Yao, X.-L. Gong and L. Chen, *Chin. J. Chem. Phys.*, 2008, **21**, 87–92.
17 J. Wu, X. Gong, L. Chen, H. Xia and Z. Hu, *J. Appl. Polym. Sci.*, 2009, **114**, 901–910.
18 H. Böse and R. Röder, *J. Phys.: Conf. Ser.*, 2009, **149**, 012090.
19 A. Boczkowska and S. F. Awietjan, *J. Mater. Sci.*, 2009, **44**, 4104–4111.
20 A. V. Chertovich, G. V. Stepanov, E. Y. Kramarenko and A. R. Khokhlov, *Macromol. Mater. Eng.*, 2010, **295**, 336–341.
21 G. Stepanov, A. Chertovich and E. Kramarenko, *J. Magn. Magn. Mater.*, 2012, **324**, 3448–3451.
22 K. Danas, S. Kankanala and N. Triantafyllidis, *J. Mech. Phys. Solids*, 2012, **60**, 120–138.
23 D. Y. Borin and G. V. Stepanov, *J. Optoelectron. Adv. Mater.*, 2013, **15**, 249–253.
24 Y. L. Raikher and O. V. Stolbov, *Tech. Phys. Lett.*, 2000, **26**, 156–158.
25 L. Borcea and O. Bruno, *J. Mech. Phys. Solids*, 2001, **49**, 2877–2919.
26 S. V. Kankanala and N. Triantafyllidis, *J. Mech. Phys. Solids*, 2004, **52**, 2869–2908.
27 M. R. Jolly, J. D. Carlson and B. C. Muñoz, *Smart Mater. Struct.*, 1996, **5**, 607–614.
28 L. C. Davis, *J. Appl. Phys.*, 1999, **85**, 3348–3351.
29 Y.-S. Zhu, X.-L. Gong, H. Dang, X.-Z. Zhang and P.-Q. Zhang, *Chin. J. Chem. Phys.*, 2006, **19**, 126–130.
30 Y. Han, W. Hong and L. E. Faidley, *Int. J. Solids Struct.*, 2013, **50**, 2281–2288.
31 D. Ivaneyko, V. P. Toshchevikov, M. Saphiannikova and G. Heinrich, *Macromol. Theory Simul.*, 2011, **20**, 411–424.
32 D. Ivaneyko, V. Toshchevikov, M. Saphiannikova and G. Heinrich, *Condens. Matter Phys.*, 2012, **15**, 33601.
33 A. Y. Zubarev, *Soft Matter*, 2012, **8**, 3174–3179.
34 A. Y. Zubarev, *Soft Matter*, 2013, **9**, 4985–4992.
35 L. D. Landau and E. M. Lifshitz, *The classical theory of fields (Course of theoretical physics series)*, Butterworth-Heinemann – Amsterdam, 1980, vol. 2, p. 402.
36 L. D. Landau, L. P. Pitaevskii and E. M. Lifshitz, *Electrodynamics of Continuous Media (Course of Theoretical Physics Series)*, Butterworth-Heinemann – Amsterdam, 1984, vol. 8.
37 J. D. Jackson, *Classical electrodynamics*, John Wiley & Sons, Inc., New York, 3rd edn, 1998, p. 832.
38 R. Feynman, R. Leighton and M. Sands, *The Feynman Lectures on Physics*, Addison-Wesley, London, 1964, p. 550.
39 C. W. Macosko, *Rheology: Principles, Measurements, and Applications*, Wiley-VCH, 1994, p. 533.
40 R. Christensen, *Mechanics of composite materials*, Dover publications, 2005, p. 384.
41 J. Domurath, M. Saphiannikova, G. Ausias and G. Heinrich, *J. Non-Newtonian Fluid Mech.*, 2012, **171–172**, 8–16.
42 T. A. Vilgis, G. Heinrich and M. Klüppel, *Reinforcement of polymer nano-composites: Theory, experiments and applications*, Cambridge University Press, Cambridge – New York, 2009, p. 209.
43 K. Morozov, M. Shliomis and H. Yamaguchi, *Phys. Rev. E: Stat., Nonlinear, Soft Matter Phys.*, 2009, **79**, 040801.
44 A. Zubarev, *Physica A*, 2013, **392**, 4824–4836.
45 G. V. Stepanov, S. S. Abramchuk, D. A. Grishin, L. V. Nikitin, E. Y. Kramarenko and A. R. Khokhlov, *Polymer*, 2007, **48**, 488–495.
46 G. V. Stepanov, D. Y. Borin, Y. L. Raikher, P. V. Melenev and N. S. Perov, *J. Phys.: Condens. Matter*, 2008, **20**, 204121.